J. Membrane Biol. 106, 47–55 (1988)

The Journal of
Membrane Biology

Gating Behaviors of a Voltage-Dependent and Ca^{2+}-Activated Cation Channel of Yeast Vacuolar Membrane Incorporated into Planar Lipid Bilayer

Manabu Tanifuji*, Masayuki Sato, Yoh Wada†, Yasuhiro Anraku†, and Michiki Kasai
Department of Biophysical Engineering, Faculty of Engineering Science, Osaka University, Toyonaka, Osaka 560, Japan, and
†Department of Biology, Faculty of Science, University of Tokyo, Hongo, Tokyo 113, Japan

Summary. A voltage-dependent and Ca^{2+}-activated cation channel found in the vacuolar membrane of the yeast, *Saccharomyces cerevisiae*, was incorporated into planar lipid bilayer and its gating characteristics were studied at the macroscopic and single-channel levels. The open-channel probability at steady state, which was estimated by the macroscopic current measurement, gave a maximum value at −10 mV and decreased in a graded fashion as the voltage became more positive or more negative. The steady-state voltage dependence was explained by assuming two independent gates, which had different rate constants and opposite voltage dependence. The fast-responding gate opened when the voltage of the *cis* side (the side to which the vesicles were added) was made more negative and the slow-responding gate behaved in the opposite direction. Relatively high concentrations of Ca^{2+}, about 1 mM, were required on the *cis* side for opening the slow gate in a voltage-dependent manner. DIDS increased the open-channel probability of the fast gate when added to the *cis* side, but was ineffective on the slow gate.

Key Words vacuole · lipid bilayer · K-channel · single channel · DIDS · yeast · *Saccharomyces cerevisiae* · Ca^{2+} activation

Introduction

In an earlier paper (Wada et al., 1987), we found that a cation-selective channel exists in vacuolar membranes[1] of the yeast, *Saccharomyces cerevisiae*. We discussed that the vacuolar channel seems to be important for the vacuolar functions, especially in relation to several transport systems in the vacuolar membrane including an H^+-ATPase (Kakinuma, Ohsumi & Anraku, 1981). Particularly, the gating properties were very interesting because of their uniqueness. The open-channel probability was dependent on applied voltage, and the gating fluctuation was completely suppressed by decreasing Ca^{2+} concentration on the *cis* side (the side to which vesicles were added). The macroscopic conductance decreased as the voltage of the *cis* side became more positive, while the channel was activated when Ca^{2+} concentration was increased. When the interaction of ions with voltage dependent gates is studied, the relation between the effective side of ions and the direction of voltage dependence is important. For example, the open-channel probability of the Ca^{2+}-activated K^+ channels increased when positive voltage was applied to the Ca^{2+}-added side (Barrett, Magleby & Pallotta, 1982; Latorre, Vergara & Hidalgo, 1982; Moczydlowski & Latorre, 1983). In this case, Ca^{2+} binding to the channel raised the open-channel probability (Moczydlowski & Latorre, 1983). A similar interpretation was made for the voltage-dependent blockage of the channel by ions (Woodhull, 1973; Coronado & Miller, 1979). In the case of the vacuolar membrane channel, however, the direction of the voltage dependence was opposite to the Ca^{2+}-effective side. Therefore, the relation between voltage dependence and Ca^{2+} requirement could not be interpreted by the above mentioned model in our case.

In this paper voltage dependence of gating was extensively studied. We found a slow decreasing phase of open-channel probability at negative voltages. This result suggests the existence of two kinds of gates with different rate constants and opposite voltage dependence. The fast-responding gate closed when the voltage of the Ca^{2+} side was made more positive, while the slow-responding gate behaved in the opposite direction (that is, the slow-responding gate opened with positive voltages). The slow gate, which resembled the gate of the Ca^{2+}-

* *Present address:* National Institute for Physiological Sciences, Myodaiji, Okazaki 444, Japan.

[1] *Abbreviations:* DIDS, 4,4′-diisothiocyanostilbene-2,2′-disulfonic acid; EGTA, Ethyleneglycol-bis(2-aminoethylether)-N,N,N′,N′-tetraacetic acid; VM, vacuolar membrane

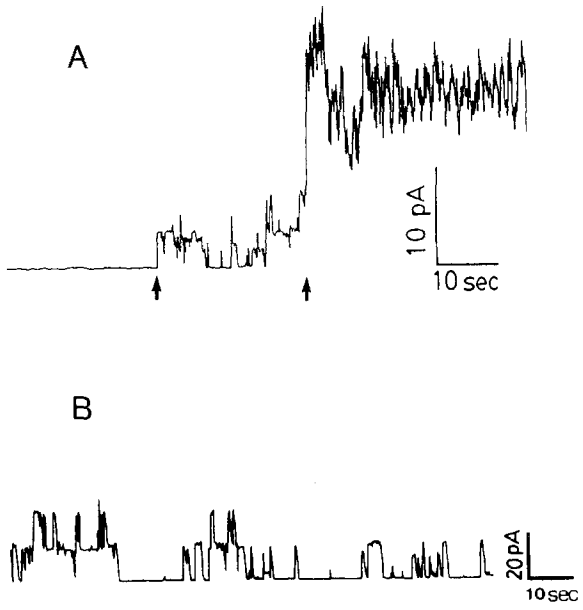

Fig. 1. Current increase of a planar bilayer after the addition of *VM* vesicles. (*A*) Both sides of membrane contained 300 mM KCl and 5 mM HEPES-tris (pH 7.2), and in addition, the *cis* side contained 1 mM $CaCl_2$. Holding potential was −10 mV. The arrows in the trace show sudden current increases that correspond to fusion events. Single-channel current fluctuations are seen between the two arrows. Current increase was upward. (*B*) Single-channel fluctuations observed under the same solution condition except that 15 mM HEPES-tris (pH 7.2) was used. Holding potential was +40 mV. Channel opening is upward. Trace *A* is the same as used in the previous paper (Wada et al., 1987)

activated K^+ channels, required Ca^{2+} for opening, and the gating was consistent with voltage-dependent activation. Further, the fast gate was found to be locked in the open state by DIDS, a K^+ channel opener (Inoue, 1986; Sokabe, 1986), whose effect was independent of the Ca^{2+} requirement for opening the channel. From these results, the gating mechanism of the channel appears to be based on two independent gates coexisting in series: Ca^{2+}-activated slow-responding gate and DIDS-sensitive fast-responding gate.

Materials and Methods

Chemicals

The vacuolar membrane (VM) vesicles from yeast, a haploid strain of *S. cerevisiae* X2180-1A, were prepared as described previously (Ohsumi & Anraku, 1981). They were resuspended in 0.4 M sucrose, 5 mM HEPES-Tris, at pH 7.2 and stored at −80°C. Before use, the VM vesicles were thawed at room temperature. Asolectin (Type II-S) was purchased from Sigma Chemical Co., USA, which contained some amounts of anionic lipids required for the vesicle fusion with bilayers. EGTA was purchased from Dojindo Laboratories (Kumamoto, Japan), and was neutralized by NaOH or KOH. Other reagents were commercial products of analytical grade.

Electrical

Planar bilayers were formed from an asolectin solution (14.7 mg/ml in *n*-decane), and VM vesicles were fused into the membranes. The electrical conductance of the membranes was measured by a current-to-voltage converter under voltage-clamp conditions and was recorded with a pen-recorder (VP-6537, National, Japan), which limited the time resolution of the system to about 10 Hz. Details of the system and the fusion process of membrane vesicles were shown previously (Tanifuji, Sokabe & Kasai, 1987). The solutions used were composed of 300 mM KCl buffered with 5 mM HEPES-Tris, at pH 7.2, unless otherwise specified.

The number of channels incorporated into planar bilayers were controlled by the amount of VM vesicles added to the solution. When 10–50 channels were incorporated into the membrane, the macroscopic measurement was carried out. On the contrary, the single-channel current fluctuations were observed when one or two channels were incorporated. The *cis* side of the membrane was defined as the side to which VM vesicles were added, and the *trans* side was defined as the opposite side. The voltage across the membrane was defined with respect to the *trans* side. Experiments were carried out at room temperature (25 ± 2°C).

Results

Fusion of Vacuolar Membrane Vesicles with Planar Bilayers

Figure 1*A* shows a current increase observed when the vesicles were added to the *cis* side. Each side of the membrane contained 300 mM KCl and an extra 1 mM $CaCl_2$ was added to the *cis* side. The current trace consists of open-close fluctuations of the channel and current increases induced by fusion events. The fusion events could be discriminated from current fluctuations by their sudden occurrence as shown by the arrows, the amplitude of which reflects the number of channels in a single vesicle. As shown in Fig. 1, a single vesicle seemed to contain a few channels. The open-close fluctuations of the channel could be observed when a small number of channels were incorporated into planar bilayers as in the trace between the two arrows. Such single-channel traces could be easily obtained by decreasing the amount of vesicles applied to the solution (Fig. 1*B*). Figure 1*B* shows current fluctuations between the multiples of a unit size. The unit size, which is referred to as single-channel current, was linearly related to applied voltages, and the single-channel conductance was 435 pS as previously shown (Wada et al., 1987).

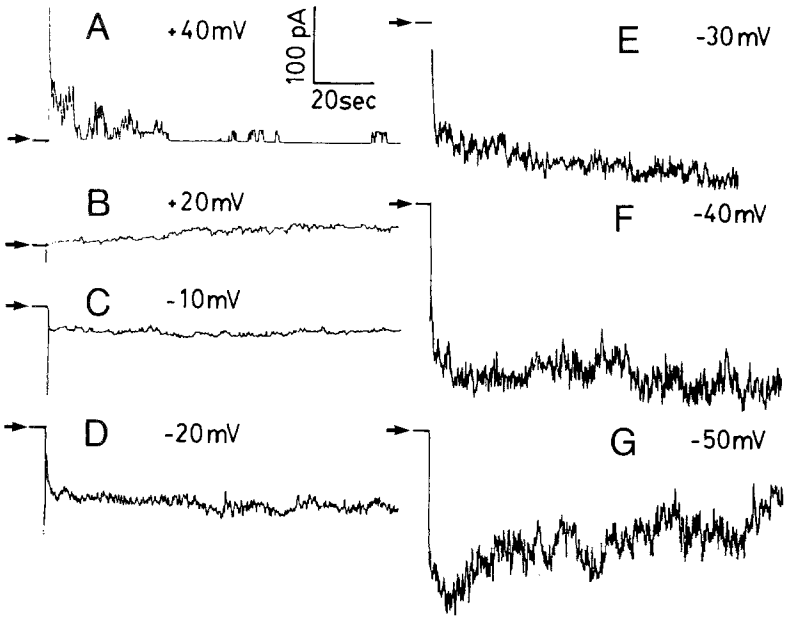

Fig. 2. Macroscopic current response to voltage jumps. Relaxation processes of currents were followed after sudden changes in voltage from +40 mV to the voltages indicated in *B–G*. Before the voltage jumps, the membrane was held at +40 mV for 2–5 min. In trace *A* the voltage was held at −40 mV and switched to +40 mV. Current increase is upward for positive voltages and downward for negative voltages. The arrow in each trace shows the zero-current level. Solutions were the same as in Fig. 1*B*. Traces *A*, *B*, *D* and *F* are the same as used in the previous paper (Wada et al., 1987)

Voltage Dependence of the Channel Gating

In the previous paper (Wada et al., 1987), we showed that this channel was characterized by two unique properties: i) the macroscopic conductance was regulated by voltage across the membrane and ii) channel opening required Ca^{2+} on the *cis* side. Since as previously shown the single-channel conductance remained constant when voltage or Ca^{2+} concentration was changed (*see* Figs. 3 and 7), these properties were not due to the modification of the conductance pathway, but due to the modification of the gating properties. Thus, the macroscopic currents could be proportional to the open-channel probability. Figure 2 shows typical traces of macroscopic currents. The voltage was first held at +40 mV for 2–5 min, a time long enough to achieve steady state, and then turned to the voltage described in each trace (traces *B–G*). In the case of trace *A*, the voltage was held at −40 mV and then switched to +40 mV. In trace *A*, the conductance rapidly decreased to zero level from a large value. When the voltage was switched to a negative value from a positive one, the channels opened (traces *C–F*). These results suggested that the channels are closed at the positive voltage and open at the negative voltage. When the voltage was held at a large negative value (trace *G*), the rapidly increasing phase of the conductance was followed by a slow decrease, and then the current reached a steady-state level. This slowly decreasing phase became more marked as the voltage was set at more negative values as shown in Fig. 2. These two characteristics of voltage-dependent gating were also observed at the single-channel level (Fig. 3). When the applied voltage was changed from a positive to a

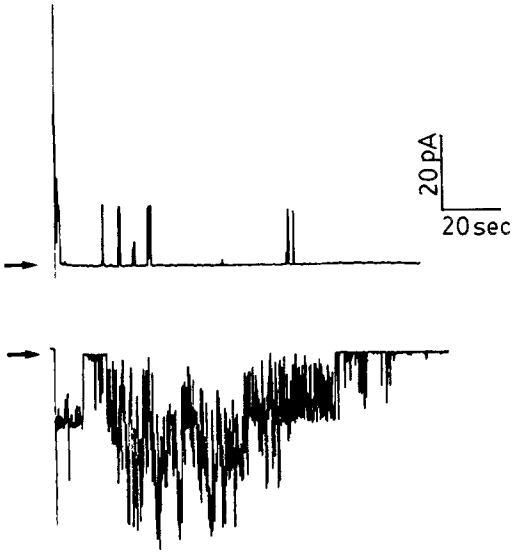

Fig. 3. Voltage dependence demonstrated at the single-channel level. The upper trace was obtained when the voltage was switched to +40 mV after having been held at −40 mV for about 30 sec, which was enough to reach the maximum conductance. The lower trace shows the current fluctuations when the voltage was switched to −40 mV after having been held at +40 mV for 2 min. Since these traces were obtained from the same membrane, the same number of channels should be present. The arrows indicate zero-current level, and current increase was upward in the upper trace and downward in the lower trace. Solution was the same as in Fig. 1*B*

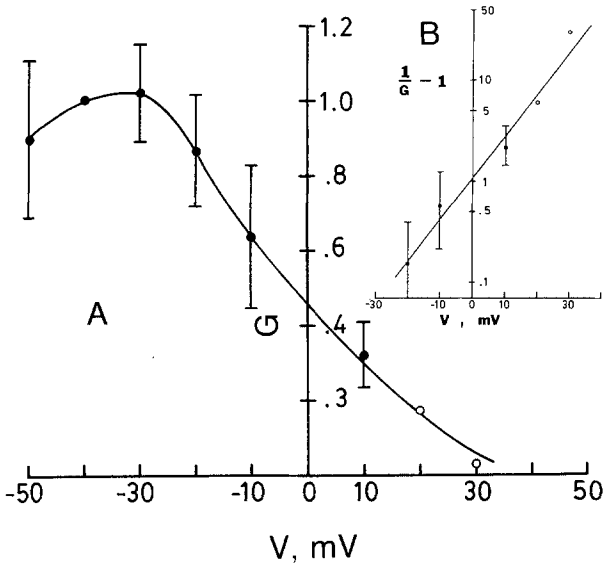

Fig. 4. *G–V* relationship of peak current. Macroscopic currents were obtained from experiments similar to that shown in Fig. 2. (*A*) Amplitudes of the maximum currents at each trace were determined and the conductances were plotted against the voltages. The conductances were normalized to the value at −40 mV. Filled circles show the means ± SD obtained from at least six measurements, and open circles show the data from single measurements. (*B*) A semilogarithmic plot of $1/G - 1$ against the voltage

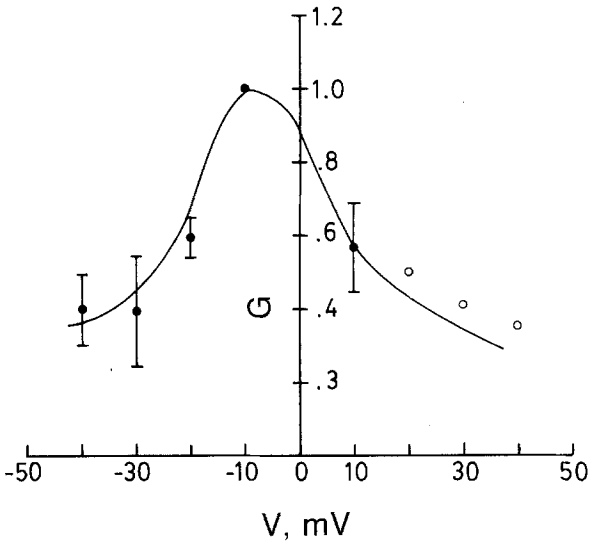

Fig. 5. Steady-state *G–V* relationship. Experiments similar to those in Fig. 2 were carried out. The steady-state conductance was measured after holding at each voltage for 15–20 min, which was enough to reach the steady state. Conductance *G* indicates the normalized value to the conductance at −10 mV. Filled circles show the means ± SD obtained from at least four measurements, and open circles show the data from single measurements. Solution was the same as in Fig. 1*B*

negative value, open-close fluctuations increased and then decreased, and when turning to the opposite direction the fluctuation disappeared immediately. Figure 3 also clearly demonstrates that the single-channel current was kept constant and only the open-channel probability changed with the change in voltage.

These observations suggest the existence of two types of gating processes: a rapidly closing process at positive voltages and a slowly closing one at negative voltages. To analyze the gating processes precisely, the peak currents and the steady-state currents were determined from macroscopic experiments similar to that shown in Fig. 2. The steady-state current was attained by waiting for 15–20 minutes at each voltage. Figure 4 shows the voltage dependence of the peak currents, where the conductance is high at negative voltages and decreases in a graded fashion as the applied voltage becomes more positive. A slight decrease in conductance is seen at −50 mV, which might be due to the effect of the slowly decreasing phase, remarkable at large negative voltages (Fig. 2*G*).

The voltage dependence shown in Fig. 4 can be analyzed by a model, assuming charge movement in the transition between a single open state and a single closed state (Ehrenstein & Lecar, 1977). According to the model, the equilibrium constant for open and closed states, $K(V)$, is given by

$$K(V) = K(0) \exp(-zFV/RT) \quad (1)$$

where z is the number of charge moves from the *trans* side to the *cis* side when the channel opens, and $K(0)$ is the equilibrium constant at zero voltage. The equilibrium constant was determined experimentally by using the following relation

$$K(V)^{-1} = 1/G - 1 \quad (2)$$

where G is the relative conductance. Figure 4*B* shows that the result satisfies the above assumption, and the values for z and $K(0)$ were 2.42 and 0.91, respectively.

The voltage dependence of the steady-state conductance is shown in Fig. 5, which was attained with a relatively slow time course as previously shown in Figs. 2 and 3. In addition to the decreasing phase at positive voltages, decrease in conductance at negative voltages appeared. As a result, the *G–V* relationship of the steady-state conductance gave a bell shaped curve, the peak of which appeared at −10 mV.

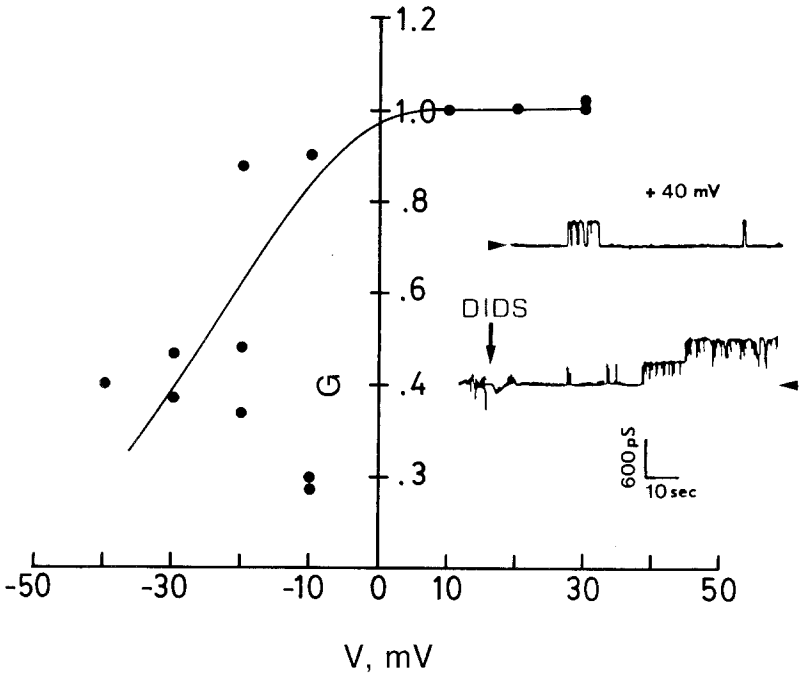

Fig. 6. Effect of DIDS on the steady-state *G–V* relationship. Experiments similar to those in Fig. 2 were carried out. Twenty μl of 20-mM DIDS (final concentration about 0.1 mM) was added to the *cis* side, and the steady-state conductance was measured at various voltages. Solution was the same as in Fig. 1*B*. Relative conductance, *G*, indicates the normalized value to the conductance at +10 mV, which gave the maximum conductance. Filled circles were obtained from a single measurement. The conductance trace shows the effect of DIDS on the single-channel level. Addition of DIDS is shown by the arrow. Holding potential was +40 mV. Other conditions were the same as in the macroscopic measurements. The arrow heads indicate zero-conductance level

Effect of DIDS on Gating

For further characterization of the two gates, several drugs that may modify the gates were used. One of the stilbene derivatives, DIDS, selectively modified one of the gates (Fig. 6). When 0.1 mM of DIDS was added to the *cis* side, rapidly closing channels began to open in a staircase fashion without a change in the single-channel conductance at the holding potential of +40 mV (Fig. 6 inset). At the negative voltage range, however, such an effect of DIDS was not observed. This observation indicated that DIDS raised the open-channel probability or locked the channel in the open state at the positive voltage. Figure 6 shows the steady-state *G–V* relationship in the presence of DIDS, which is a monotonous function of voltage. Comparing this with the *G–V* relationship without DIDS (Fig. 5), it is clear that the macroscopic conductance was obviously raised by DIDS at positive voltages, but remained unchanged at negative voltages. The observation suggests that only the rapidly closing process characterized by Fig. 4 was modified by DIDS. When DIDS was added to the *trans* side, no effect was observed (*data not shown*).

Ca^{2+} Dependence

The effect of Ca^{2+} on the gating behavior was also studied. Figure 7 shows a typical result of the effect of Ca^{2+}. When the Ca^{2+} concentration of the *cis* side was lowered from 1 mM to 0.3 mM, the open-channel probability significantly decreased while the single-channel conductance was left unchanged. Application of Ca^{2+} to the *cis* side showed recovery of open-channel probability, but such recovery could not be observed when Ca^{2+} was added to the *trans* side (*data not shown*). An addition of Mg^{2+} to the *cis* side could not recover the open-channel probability, but further addition of Ca^{2+} recovered it (Fig. 8).

The concentration of Ca^{2+} required for channel opening is shown in Fig. 9. Although the data are insufficient for detailed analysis, the result shows the requirement of relatively high concentrations of Ca^{2+}, about 1 to 2 mM.

Relationship Between Ca^{2+} Requirement and DIDS Effect

It was shown that two types of voltage-dependent gating processes existed; the fast-responding one was locked at the open state by DIDS and Ca^{2+} was required for opening it. Now the question is to clarify which types of gates require Ca^{2+}. To answer this question, the effect of Ca^{2+} and DIDS on the voltage dependence was studied. Figure 10 shows the effect of Ca^{2+} on the steady-state *G–V* relationships in the absence (*A*) and presence (*B*) of DIDS. Before the addition of DIDS, Ca^{2+} did not modify the *G–V* relation in the positive voltage region, but did so in the negative region (Fig. 10*A*). In the pres-

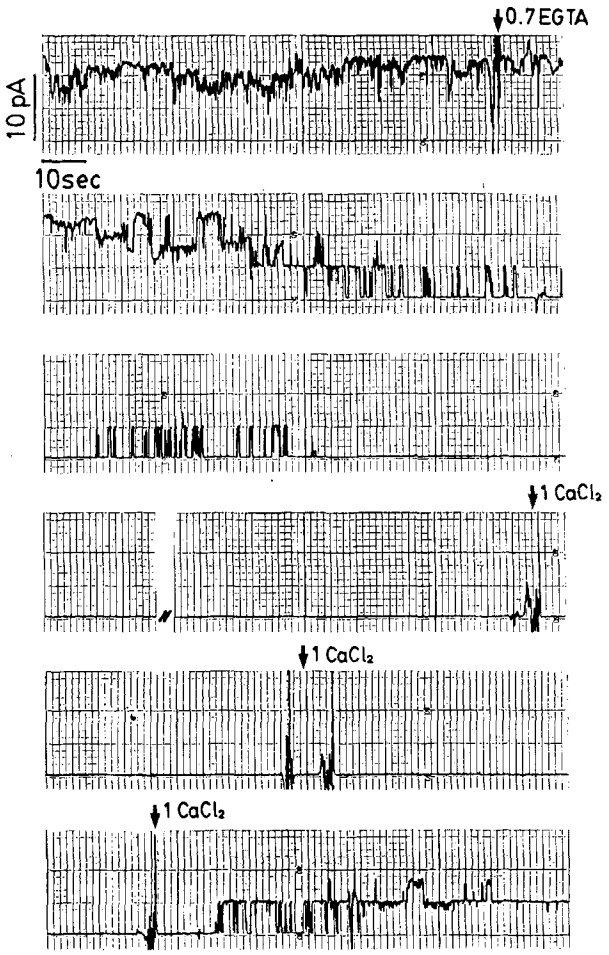

Fig. 7. Effect of Ca^{2+} on gating. At the points shown in the figure, EGTA and Ca^{2+} were added to the *cis* side. Their concentrations are indicated in millimolar; 0.7 mM EGTA produced 0.3 mM of free Ca^{2+}. Further application of 3 mM $CaCl_2$ produced about 3 mM of free Ca^{2+}. A pair of slashes in the trace means that several minutes passed where no current fluctuation was observed. The initial solution was the same as in Fig. 1*B*. Holding potential was −10 mV. Channel opening was upward

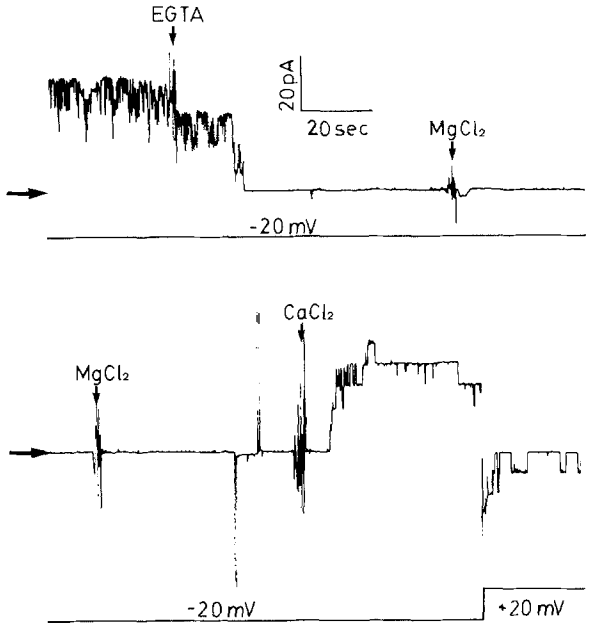

Fig. 8. Effect of Mg^{2+} demonstrated at the single-channel level. As shown by the arrow, an addition of 1 mM EGTA to the *cis* side resulted in closing the channels. After that 5 mM $MgCl_2$ was added twice to the *cis* side, but no current fluctuation was observed. Further application of 1 mM $CaCl_2$ caused recovery of current fluctuations and the *G–V* relation was the same as in Fig. 4. The initial solution was the same as in Fig. 1*B*. Holding potential is shown under the current trace. The arrows indicate zero-current level, and channel opening was upward at negative voltage and downward at positive voltage

ence of DIDS the channel becomes open at positive voltages (similar to the results in Fig. 6). Ca^{2+} did not affect the gate at the positive voltage, but increased the open-channel probability at the negative voltage region (Fig. 10*B*). This result indicates that the channel opens only when two types of gates are open and that the fast-responding gate, which closes at the positive voltages, is locked in the open state by DIDS and the slow-responding gate, which closes at negative voltages, requires Ca^{2+} for opening. When Ca^{2+} concentration was decreased to micromolar range, the channel closed completely even in the presence of DIDS (*data not shown*). These results indicate that the channel activation with increasing voltage observed in the negative voltage

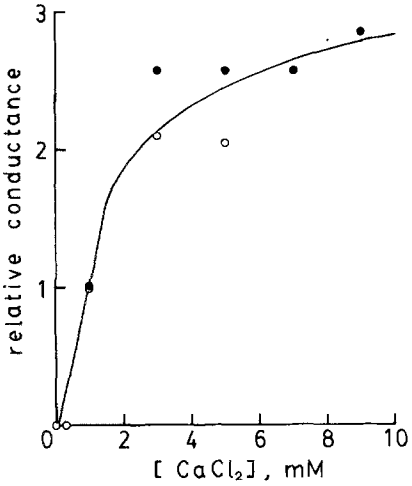

Fig. 9. Dependence of conductance on Ca^{2+}. Free Ca^{2+} concentration in the *cis* solution was controlled by the addition of EGTA or $CaCl_2$. The solution was initially the same as in Fig. 1*B*. Relative conductance indicates the normalized value to the conductance in the solution containing 1 mM $CaCl_2$. Before changing Ca^{2+} concentration, the membranes were held at −10 mV for 1–3 min, which was enough to reach the steady-state value. Holding potentials were −10 mV. Filled circles were obtained from macroscopic currents and open circles were obtained from time-averaged single-channel currents. Potential shifts induced by asymmetric addition of Ca^{2+} were not taken into account

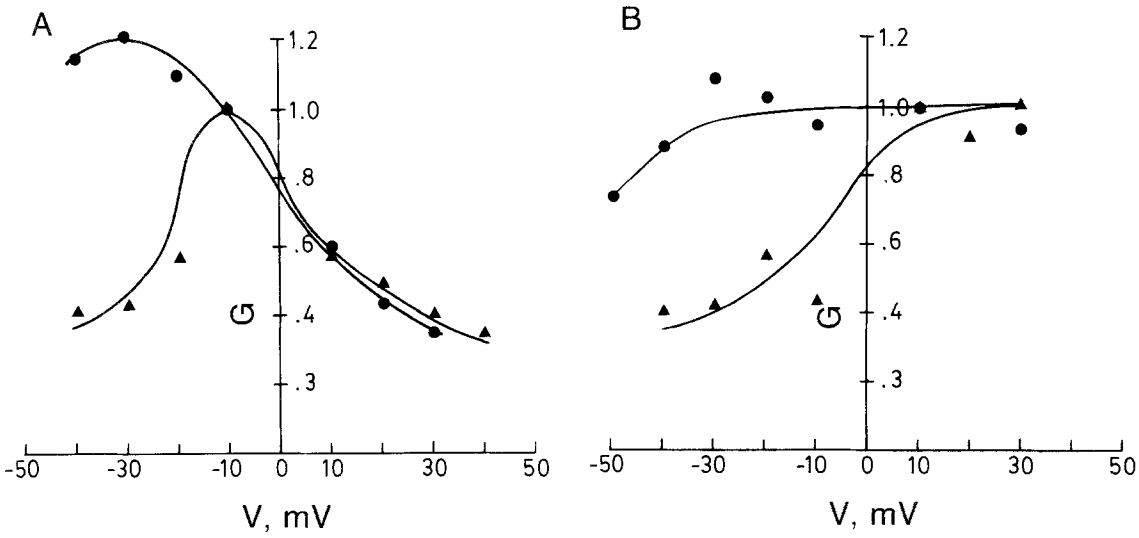

Fig. 10. Effect of Ca^{2+} and DIDS on steady-state G–V relationship. Experiments similar to those in Fig. 5 were carried out in the absence and presence of DIDS. Ca^{2+} was added to both sides of the chamber in order to remove the effect of surface potential: (▲) 1 mM Ca^{2+} and (●) 2 mM Ca^{2+}. Other conditions were the same as those in Fig. 5. (*A*) G–V relation in the absence of DIDS. Steady-state conductances without DIDS were the mean values taken for Fig. 5. Relative conductance, G, indicates the normalized value to the conductance at −10 mV. (*B*) G–V relationship in the presence of DIDS on the *cis* side (final concentration was 0.1 mM). Relative conductance, G, indicates the normalized value to the conductance at +10 mV

region was shifted to the right of the voltage axis when the Ca^{2+} concentration was decreased. Further, these results were supported by single-channel observation (*data not shown*).

Discussion

Current traces, both in single-channel recordings (Fig. 3) and in macroscopic measurements (Fig. 2), suggested the existence of two types of gating processes: the gating process responding fast to applied voltages (type F) and the one responding slowly (type S). The voltage dependence of type F could be estimated from peak currents obtained in Fig. 2, since the time to reach the peak was short enough for type S not to respond. The voltage dependence of type S was estimated from the steady-state G–V relationship (Fig. 5). As a result, open-channel probability of the type F gate was found to decrease in a graded fashion as the voltage becomes more positive. Further, Fig. 4 suggested that voltage dependence of type F could be explained by Eq. (1). On the contrary, taking into account that the peak conductance did not change significantly in the negative voltage region (Fig. 4), and assuming a monotonous function for the G–V relationship of type S as seen in the case of type F, it is suggested that the open-channel probability of type S increases as the applied voltage becomes more positive. Further characteristics of these gates are discussed below.

Effect of DIDS on Gating

In this study, one of the stilbene derivatives, DIDS, was found to act as the channel opener, as shown in the single-channel trace (Fig. 6). This kind of effect of stilbene derivatives has also been reported on some voltage-gated K^+ channels (Inoue, 1986; Sokabe, 1986). Sokabe (1986) showed that voltage-gated K^+ channels of sarcoplasmic reticulum, which shows the monotonous voltage dependence given by Eq. (1), lose their voltage dependence, as DIDS lock the channel in the open state at any voltage. However, in the case of the vacuolar membrane channel, the effect was complicated. When DIDS was added, the open-channel probability was raised in the positive voltage range, but not in negative voltage range. The result suggested that DIDS locked only the type F gate in the open state (Fig. 6), but not the type S gate. If so, the voltage dependence of the type S gate could be estimated by the G–V relationship when DIDS existed (Fig. 6). The result was consistent with the voltage dependence of the type S gate postulated above from the steady-state voltage dependence. In some cases, flickering behavior was observed when DIDS was added (*data not shown*). This may attribute the scatter of the data at negative voltages in Fig. 6.

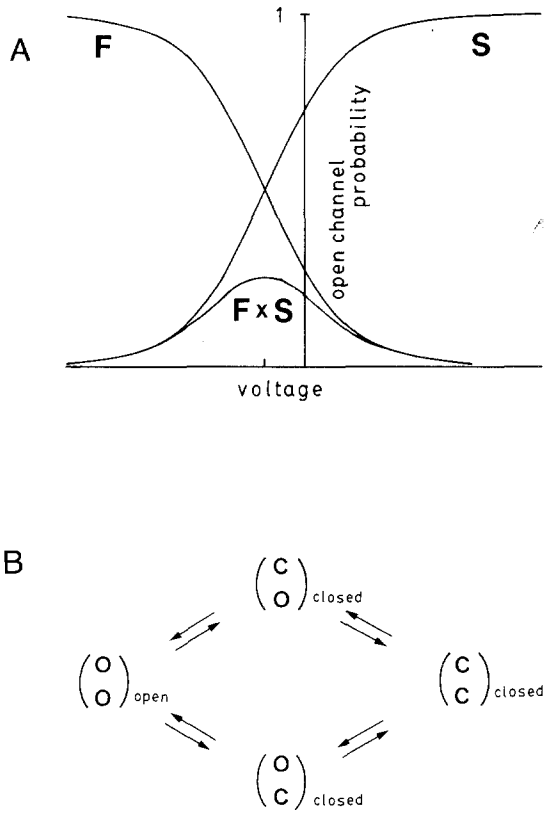

Fig. 11. A model for gating of the vacuolar membrane channel. (*A*) Voltage dependences of two types of gating processes are shown schematically, where *F* and *S* indicate type F and S gates. Multiplication of the open-channel probability of type F by that of type S gives the steady-state voltage dependence of open-channel probability shown by $F \times S$. (*B*) Schematic representation of the states of the channel. Because of two independent gates, the channel consists of four states, each of which is determined by combination of the states of two gates, namely, open (*O*) or closed (*C*). The states are expressed as a matrix, whose elements mean the state of gate *F* (upper) and gate *S* (lower). The channel opens only when both gates are open

Ca^{2+} Activation

Ca^{2+} activation was observed at negative voltages in the absence or in the presence of DIDS (Fig. 10*A,B*). Further, channels were completely closed when EGTA was added in both cases (*data not shown*). These results can be explained by assuming that the type S gate is regulated by Ca^{2+}, which is consistent with the effect of DIDS on the type F gate. It is still possible to imagine that besides the type S gate there is another gate that is regulated by Ca^{2+} in a voltage-independent way. However, this is not the case because increasing concentrations of Ca^{2+} shift the voltage dependence of the steady-state conductance (Fig. 10*A*). Furthermore, a similar shift of voltage dependence by Ca^{2+} was also observed when DIDS was added (Fig. 10*B*). Thus we can conclude that the type S gate is regulated by Ca^{2+}, and increasing Ca^{2+} concentration shifts the voltage dependence of this gate to negative voltage. Such a Ca^{2+}-dependent shift of voltage dependence was observed in Ca^{2+}-activated K^+ channels, and was precisely studied by several researchers (Barrett et al., 1982; Methfessel & Boheim, 1982; Wong & Lecar, 1982; Moczydlowski & Latorre, 1983). They observed that open-channel probability was raised when the potential of the side where Ca^{2+} was added was made more positive. Further, the voltage dependence was shifted along the voltage axis when Ca^{2+} concentration was changed. These gating behaviors were interpreted by the voltage-dependent binding of Ca^{2+} to the channel (Moczydlowski & Latorre, 1983). In the present case, the behavior of the type S gate was similar to that of the Ca^{2+}-activated K^+ channels. However, there were some differences: the concentration of Ca^{2+} required for channel opening was quite high, and the open-close fluctuations were slower than those of other Ca^{2+}-activated K^+ channels. Further investigations, particularly of Ca^{2+} interaction with the channel, are required.

Conclusion

Our observation of the present channel leads us to the scheme shown in Fig. 11. The channel has two gating systems, type F and type S, located in series, whose properties are as follows.

Type F: (i) The gate responds relatively fast to the voltage jump. (ii) Open-channel probability decreases as the applied voltage becomes more positive (Fig. 4). (iii) Open-channel probability is raised by DIDS from the *cis* side.

Type S: (i) The gate responds relatively slowly to the voltage jump: (ii) Open-channel probability increases as the applied voltage becomes more positive. (iii) Ca^{2+} is required for opening the gate from the *cis* side. (iv) When the Ca^{2+} concentration is increased, the curve of voltage dependence shifts to the negative voltage direction, which is consistent with the notion of voltage-dependent binding of Ca^{2+}.

Recent investigation by patch-clamp techniques showed that Ca^{2+}-dependent channels also exist in vacuolar membranes isolated from sugarbeet (Hedrich & Neher, 1987). The gating characteristics, however, were not the same as the channels in the yeast. Particularly, the yeast channel required significantly higher concentrations of Ca^{2+} to open the channel under the present experimental conditions compared with the cytoplastmic Ca^{2+} concentra-

tion. This discrepancy can be explained by the possibility that the lipid composition of bilayer is largely different from that of vacuolar membrane, that some modulators of the channel are not functional in the bilayer system, or that the potential across the vacuolar membrane is largely negative in vivo, where the required Ca^{2+} concentration becomes lower as suggested by Fig. 10.

This work was supported by a Grant-in-Aid for Special Project Research on Bioenergetics to Y.A. and M.K. from the Japanese Ministry of Education, Science and Culture.

References

Barrett, J.N., Magleby, K.L., Pallotta, B.S. 1982. Properties of single calcium-activated potassium channels in cultured rat muscle. *J. Physiol. (London)* **331:**211–230

Coronado, R., Miller, C. 1979. Voltage-dependent caesium blockade of a cation channel from fragmented sarcoplasmic reticulum. *Nature (London)* **280:**807–810

Ehrenstein, G., Lacar, H. 1977. Electrically gated ionic channels in lipid bilayers. *Q. Rev. Biophys.* **10:**1–34

Hedrich, R., Neher, E. 1987. Cytoplasmic calcium regulates voltage-dependent ion channels in plant vacuoles. *Nature (London)* **329:**833–836

Inoue, I. 1986. Modification of K conductance of the squid axon membrane by SITS. *J. Gen. Physiol.* **88:**507–520

Kakinuma, Y., Ohsumi, Y., Anraku, Y. 1981. Properties of H^+-translocating adenosine triphosphatase in vacuolar membranes of *Saccharomyces cerevisiae*. *J. Biol. Chem.* **256:**10859–10863

Latorre, R., Vergara, C., Hidalgo, C. 1982. Reconstitution in planar lipid bilayers of a Ca^{2+}-dependent K^+ channel from transverse tubule membranes isolated from rabbit skeletal muscle. *Proc. Natl. Acad. Sci. USA* **79:**805–809

Methfessel, C., Boheim, G. 1982. The gating of single calcium-dependent potassium channels is described by an activation/blockade mechanism. *Biophys. Struct. Mech.* **9:**35–60

Moczydlowski, E., Latorre, R. 1983. Gating kinetics of Ca^{2+}-activated K^+ channels from rat muscle incorporated into planar lipid bilayers: Evidence for two voltage-dependent Ca^{2+} binding reactions. *J. Gen. Physiol.* **82:**511–542

Ohsumi, Y., Anraku, Y. 1981. Active transport of basic amino acids driven by a proton motive force in vacuolar membrane vesicles of *Saccharomyces cerevisiae*. *J. Biol. Chem.* **256:**2079–2082

Sokabe, M. 1986. Voltage dependent gate of a K^+ channel from sarcoplasmic reticulum in planar bilayer lipid membranes. *In:* Int. Symp. Ion Channels and Electrogenic pumps in Biomembranes (*Abstract*), M. Kasai, editor. pp. L39–50. Osaka, Japan

Tanifuji, M., Sokabe, M., Kasai, M. 1987. An anion channel of *sarcoplasmic reticulum* incorporated into planar lipid bilayers: Single-channel behavior and conductance properties. *J. Membrane Biol.* **99:**103–111

Wada, Y., Ohsumi, Y., Tanifuji, M., Kasai, M., Anraku, Y. 1987. Vacuolar ion channel of the yeast, *Saccharomyces cerevisiae*. *J. Biol. Chem.* **262:**17260–17263

Wong, B.S., Lecar, H. 1982. Single calcium-dependent potassium channels in clonal anterior pituitary cell. *Biophys. J.* **39:**313–317

Woodhull, A.M. 1973. Ionic blockade of sodium channel in nerve. *J. Gen. Physiol.* **61:**687–708

Received 15 April 1988; revised 5 July 1988